

Electronic Supplementary Information for:

Layered Hybrid Perovskite Solar Cells Based on Single-Crystalline Precursor Solutions with Superior Reproducibility

Yangyang Dang, ^{#ac} Jing Wei, ^{#b} Xiaolong Liu, ^a Xi Wang, ^b Kun Xu, ^b Ming Lei, ^{*b}
Wenping Hu, ^{*c} and Xutang Tao^{*a}

^aInstitute of Crystal Materials & State Key Laboratory of Crystal Materials,
Shandong University, No. 27 Shanda South Road, Jinan, 250100, P. R. China.

^b State Key Laboratory of Information Photonics and Optical Communications,
School of Science, Beijing University of Posts and Telecommunications, Beijing,
100876, P. R. China.

^c Tianjin Key Laboratory of Molecular Optoelectronic Sciences & Department of
Chemistry, School of Sciences, & Collaborative Innovation Center of Chemical
Science and Engineering, Tianjin University, Tianjin, 300072, P. R. China.

E-mail: txt@sdu.edu.cn; huwp@tju.edu.cn; mlei@bupt.edu.cn

Experimental Section

Figure S1. The BA_2PbI_4 and MAPbI_3 single crystals by TSSG and BSSG method, respectively.

Figure S2. Experimental and calculated X-ray diffraction (XRD) patterns of BAI , $\text{BA}_2\text{MA}_{n-1}\text{Pb}_n\text{I}_{3n+1}$ ($n=1, 3, 4$).

Figure S3. Calculated morphologies of $\text{BA}_2\text{MA}_{n-1}\text{Pb}_n\text{I}_{3n+1}$ ($n=1, 3, 4$) by Bravais–Friedel–Donnay–Harker (BFDH) method.

Figure S4. (a-c) Diagrams of layered crystal structures of $\text{BA}_2\text{MA}_{n-1}\text{Pb}_n\text{I}_{3n+1}$ ($n=1, 3, 4$) single crystals.

Figure S5. UV-vis spectra of $\text{BA}_2\text{MA}_{n-1}\text{Pb}_n\text{I}_{3n+1}$ ($n = 1, 3, 4$) single crystals. Inset: Corresponding band gaps determined by using Kubelka–Munk function.

Figure S6. PL spectra of thick $\text{BA}_2\text{MA}_{n-1}\text{Pb}_n\text{I}_{3n+1}$ ($n=1, 3, 4$) single crystals.

Figure S7. PL spectra of thin $\text{BA}_2\text{MA}_{n-1}\text{Pb}_n\text{I}_{3n+1}$ ($n= 3, 4$) single crystals

Figure S8. The TGA and DSC data of $\text{BA}_2\text{MA}_{n-1}\text{Pb}_n\text{I}_{3n+1}$ ($n=1, 3, 4$).

Figure S9. The XRD patterns and performance of solar cells with $\text{BA}_2\text{MA}_{n-1}\text{Pb}_n\text{I}_{3n+1}$ ($n=3, 4$) thin film based on conventional precursors by modified hot-casting method.

Figure S10. The pictures and PCE of FASnI_3 thin film devices based on the single-crystalline precursor solutions.

Table S1. Crystal structure parameters data of BA_2PbI_4 .

Table S2. The device parameters of black FASnI_3 solar cells based on the single-crystalline precursors.

Experimental Section

Bulk growth of high quality MAPbI₃ single crystal. To improve the quality of MAPbI₃ single crystal, the crystal growth via a regular-shape seed crystal and proper cooling rate has been adopted with the reaction of Pb(CH₃COO)₂·3H₂O and MAI in HI solution, based on the previous report.¹ The saturation temperature of the solution was measured to be 63.5 °C. Crystals were grown by cooling the solution at a rate of 1-2 °C/day. After a growing period of one month, the high quality MAPbI₃ single crystals were grown by bottom-seeded solution growth (BSSG) method in **Figure S1b**.

Single-crystal, powder and film X-ray diffractions. Single-crystal and powder X-ray diffraction measurements were depicted elsewhere [1] BA₂MA_{n-1}Pb_nI_{3n+1} (n=1, 3, 4) single crystal samples were selected and utilized for single-crystal X-ray diffraction at 293 K. Film X-ray diffractions were recorded on an X'PertMPD PRO from PANalytical equipped with a ceramic tube (Cu anode, λ/41.54060 Å), a secondary graphite (002) monochromator and a RTMS X'Celerator detector and operated in BRAGG-BRENTANO geometry. The samples were mounted without further modification, and the automatic divergence slit and beam mask were adjusted to the dimensions of the thin films. A step size of 0.008° was chosen and an acquisition time of up to 7.5 min/deg.

TGA and DSC measurements. The TGA and DSC measurements were performed on the TGA/DSC1/1600HT analyzer (METTLER TOLEDO instruments). BA₂MA_{n-1}Pb_nI_{3n+1} (n=1, 3, 4) powder samples were placed in the Al crucible, and heated at a rate of 10 °C min⁻¹ from room temperature to 800 °C under flowing N₂ gas.

UV-vis diffuse reflectance spectroscopy and PL spectra measurements. UV-vis diffuse reflectance spectroscopy was executed a Shimadzu UV 2550 spectrophotometer equipped with integrating sphere over the spectral rang 200-900 nm. A BaSO₄ plate was used as the standard. BA₂MA_{n-1}Pb_nI_{3n+1} (n=1, 3, 4) powder samples were placed and coated on the surface of BaSO₄ plate. The PL spectra of BA₂MA_{n-1}Pb_nI_{3n+1} (n=1, 3, 4) single crystals were collected using a Nikon fluorescence microscope, which gathered with a Carl Zeiss Jena LSM 780 confocal laser fluorescence microscope.

Scanning Electronic Microscope (SEM) measurements. The surface morphology of the perovskite film was characterized by SEM (Nano430, FEI). The electron beam is accelerated at 10 kV.

Fabrications and measurements of FASnI₃ solar cells. All reagents and solvents, unless otherwise specified, were purchased from Aladdin, Aldrich and J&K Scientific Ltd. and were used without further purification. PC₆₁BM was purchased from American Dyes Source, Inc. Prior to fabrication, the substrates were cleaned by sonication using detergent, deionized water, acetone, and isopropanol sequentially for every 15 min followed by 15 min of ultraviolet ozone (UV-Ozone) treatment. Then a layer of PEDOT: PSS was spin-coated onto the cleaned ITO and annealed at 140°C for 15 min. The substrates were transferred to a glovebox. Perovskite was dissolved in DMSO at a concentration of 1.3 M. The solution was kept at R.T. during the whole procedure. The solution was then spin coated on PEDOT: PSS at 4000 rpm for 60 s. A drop of chlorobenzene was dropped at 30 s. Afterwards, the as prepared films were heated at 145 °C for

15 min. An electron transporting layer (ETL) was then deposited *via* spin coating a layer of [6,6]-phenyl-C₆₁-butyric acid methyl ester (PC₆₁BM, 20 mg mL⁻¹) in chlorobenzene at 2000 rpm for 45 s. A hole-blocking layer was deposited *via* spin-coating ZnO nanoparticles in ethanol at 4000 rpm for 30 s on the top of PC₆₁BM layer. Subsequently, samples were loaded into a vacuum deposition chamber (background pressure $\approx 5 \times 10^{-4}$ Pa) to deposit a 100 nm thick Al cathode. To specify the illuminated area, we used an aperture (shadow mask) with an area of 0.06 cm², whereas the total device area defined by the overlap of the electrodes was approximately 0.12 cm².

The J - V characteristics were measured with Keithley 2400 measurement source units with the devices maintained at room temperature in glove-box. The photovoltaic response was measured under a calibrated solar simulator (Enli Technology) at 100 mW cm⁻², and the light intensity was calibrated with a standard photovoltaic reference cell.

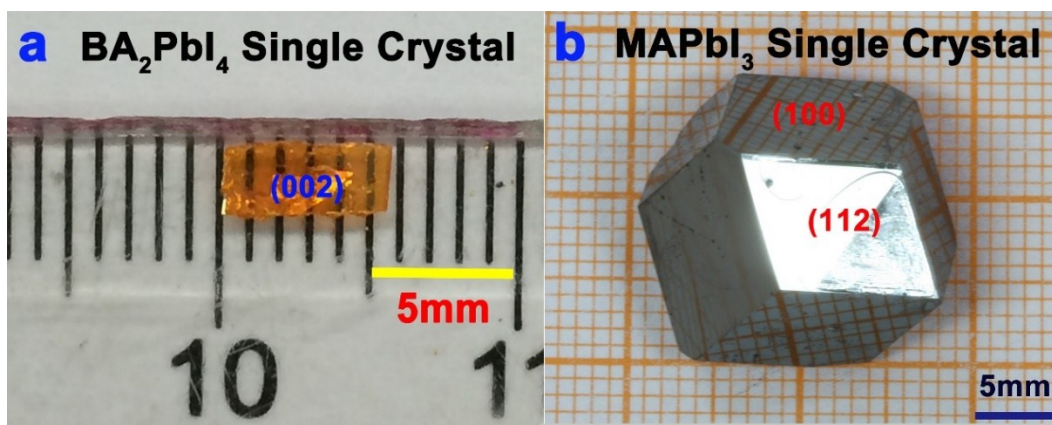


Figure S1. The BA_2PbI_4 and MAPbI_3 single crystals by TSSG and BSSG method, respectively. (a) orange colour BA_2PbI_4 single crystals; (b) high-quality MAPbI_3 single crystals.

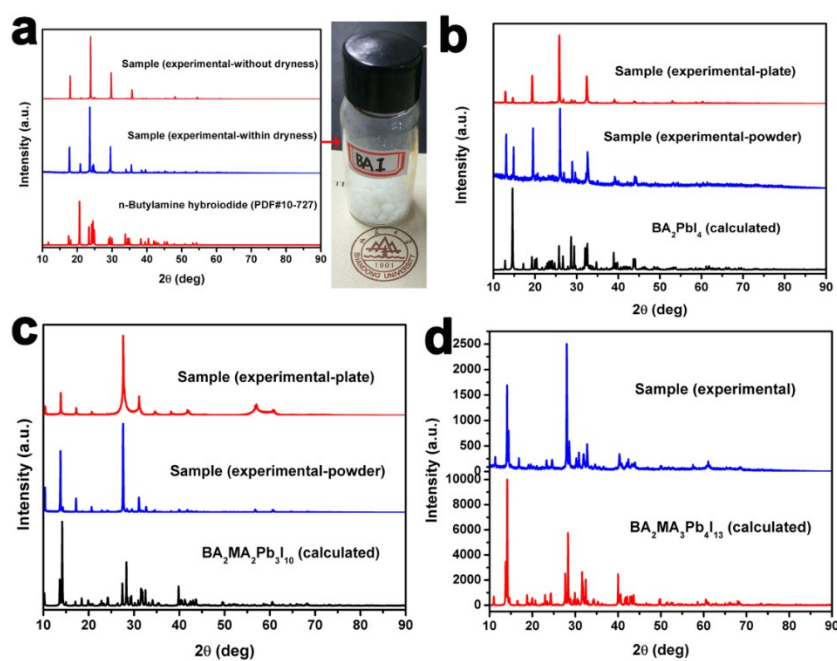


Figure S2. Experimental and calculated X-ray diffraction (XRD) patterns of BAI, BA_2PbI_4 , $\text{BA}_2\text{MA}_2\text{Pb}_3\text{I}_{10}$ and $\text{BA}_2\text{MA}_3\text{Pb}_4\text{I}_{13}$. (a) Experimental and calculated XRD patterns of BAI, Insert: the photography of BAI; (b) Experimental and calculated XRD patterns of BA_2PbI_4 ; (c) Experimental and calculated XRD patterns of $\text{BA}_2\text{MA}_2\text{Pb}_3\text{I}_{10}$; (d) Experimental and calculated XRD patterns of $\text{BA}_2\text{MA}_3\text{Pb}_4\text{I}_{13}$.

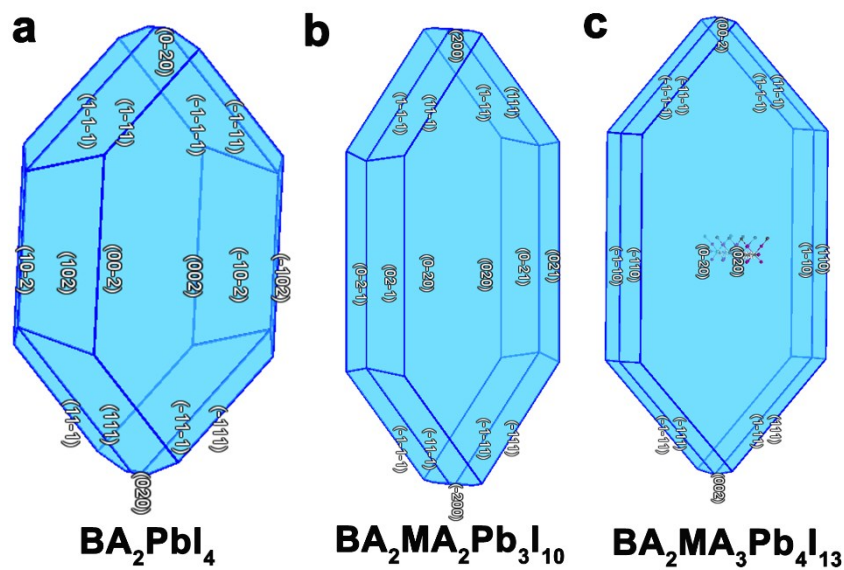


Figure S3. Calculated morphologies of BA₂MA_{n-1}Pb_nI_{3n+1} (n=1, 3, 4) by Bravais-Friedel-Donnay-Harker (BFDH) method.

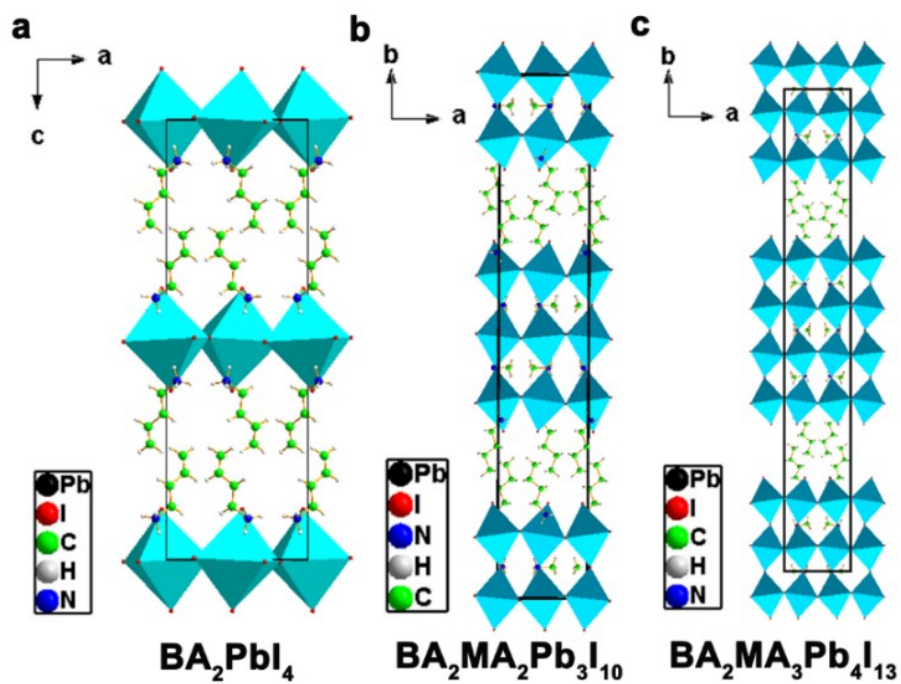


Figure S4. (a-c) Diagrams of layered crystal structures of BA₂MA_{n-1}Pb_nI_{3n+1} (n=1, 3, 4) single crystals.

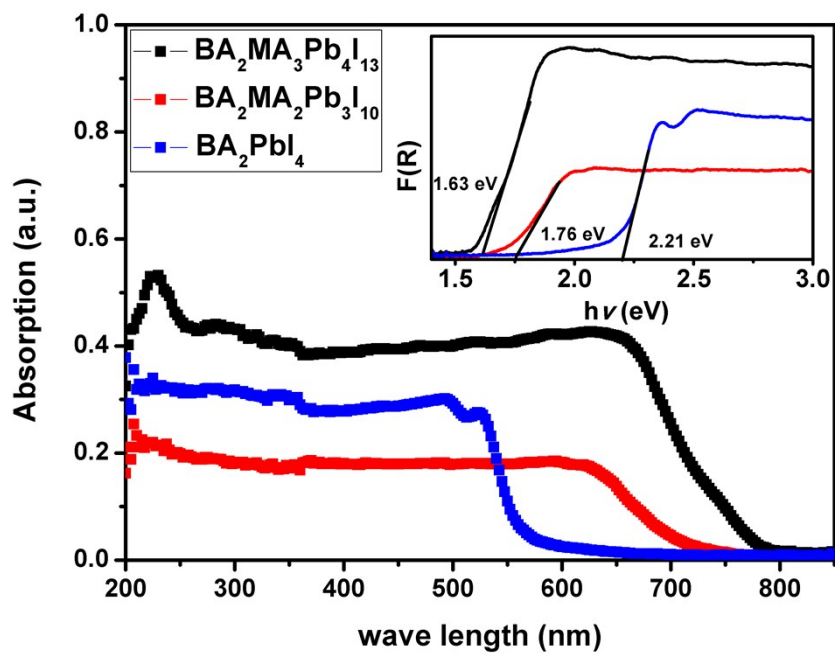


Figure S5. UV-vis spectra of $\text{BA}_2\text{MA}_{n-1}\text{Pb}_n\text{I}_{3n+1}$ ($n = 1, 3, 4$) single crystals. Inset: Corresponding band gaps determined by using Kubelka–Munk function.

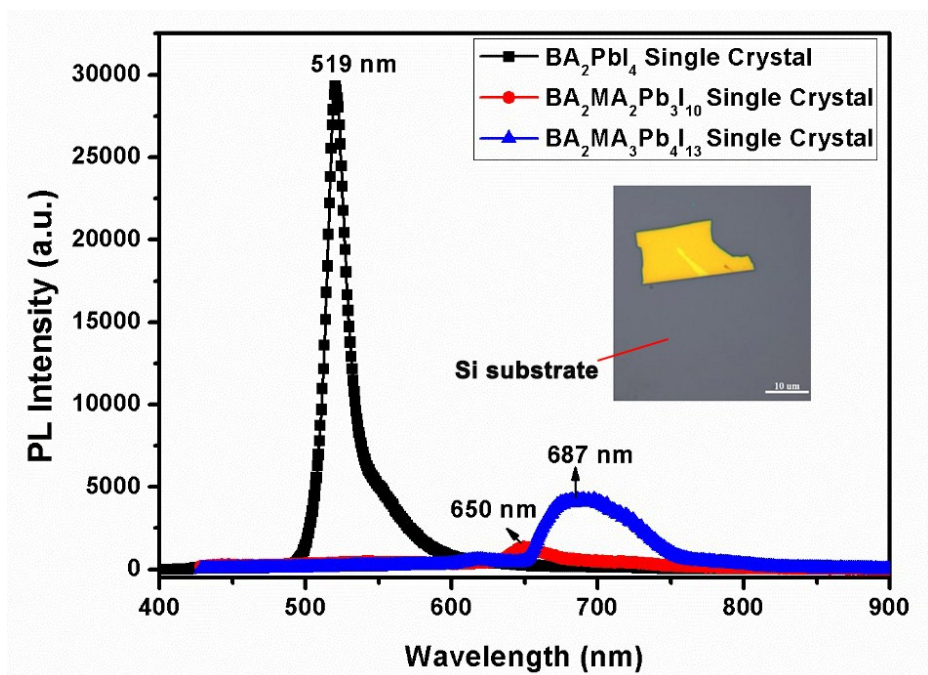


Figure S6. PL spectra of thick $\text{BA}_2\text{MA}_{n-1}\text{Pb}_n\text{I}_{3n+1}$ ($n=1, 3, 4$) single crystals.

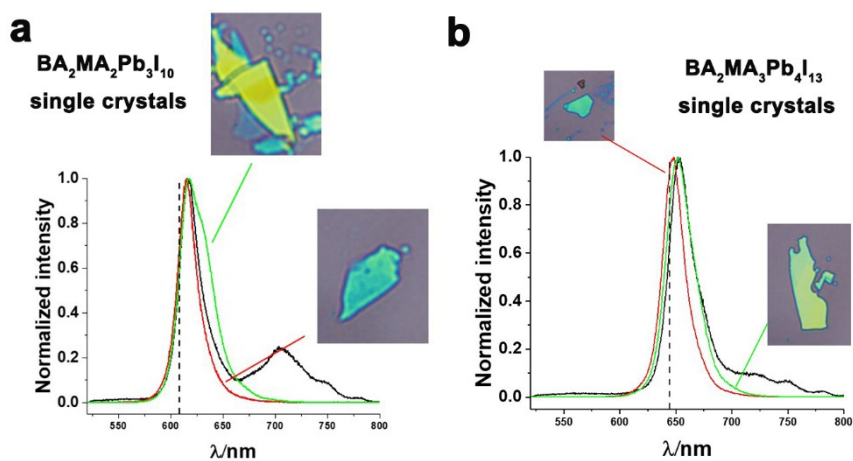


Figure S7. PL spectra of thin $\text{BA}_2\text{MA}_{n-1}\text{Pb}_n\text{I}_{3n+1}$ ($n=3, 4$) single crystals

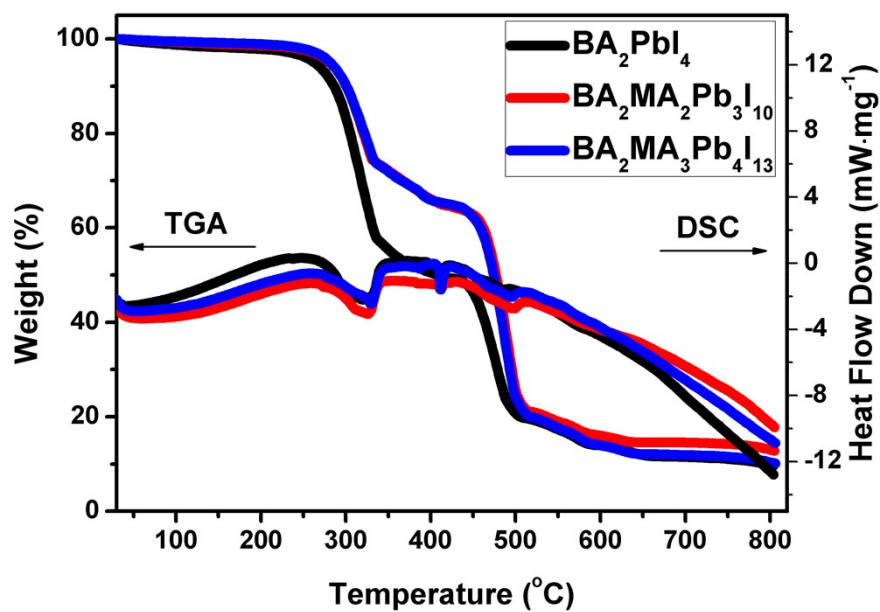


Figure S8. The TGA and DSC data of $\text{BA}_2\text{MA}_{n-1}\text{Pb}_n\text{I}_{3n+1}$ ($n=1, 3, 4$).

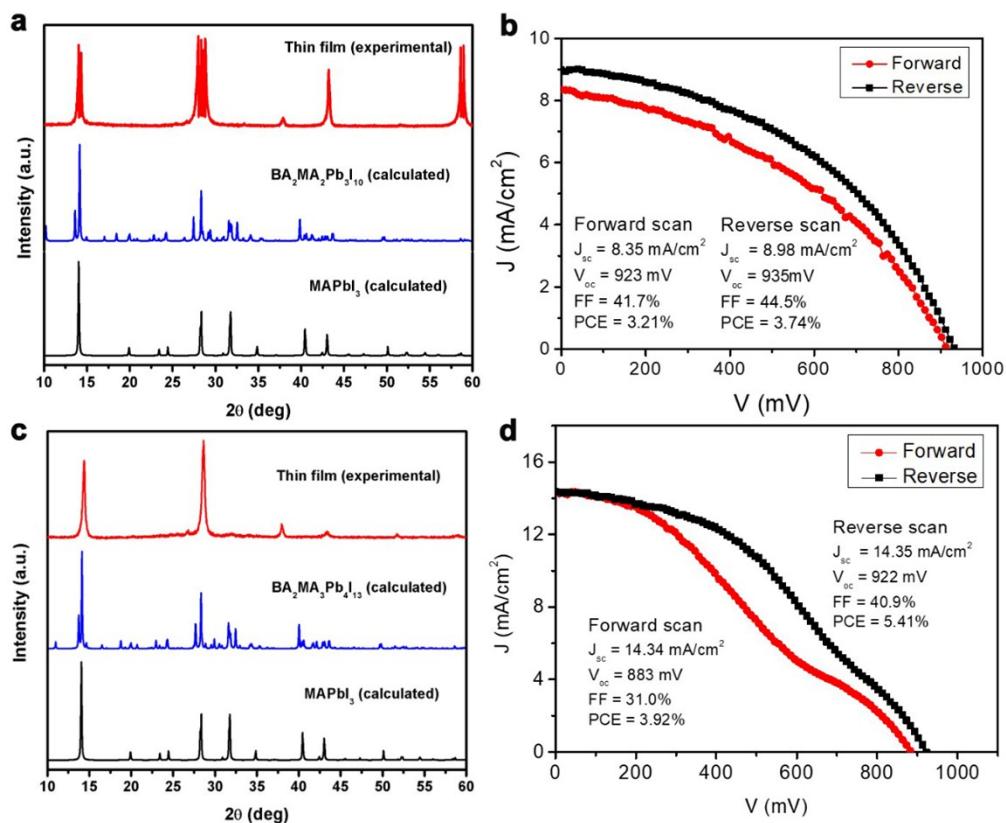


Figure S9. The XRD patterns and performance of solar cells with $\text{BA}_2\text{MA}_{n-1}\text{Pb}_n\text{I}_{3n+1}$ ($n=3, 4$) thin film based on conventional precursors by modified hot-casting method.

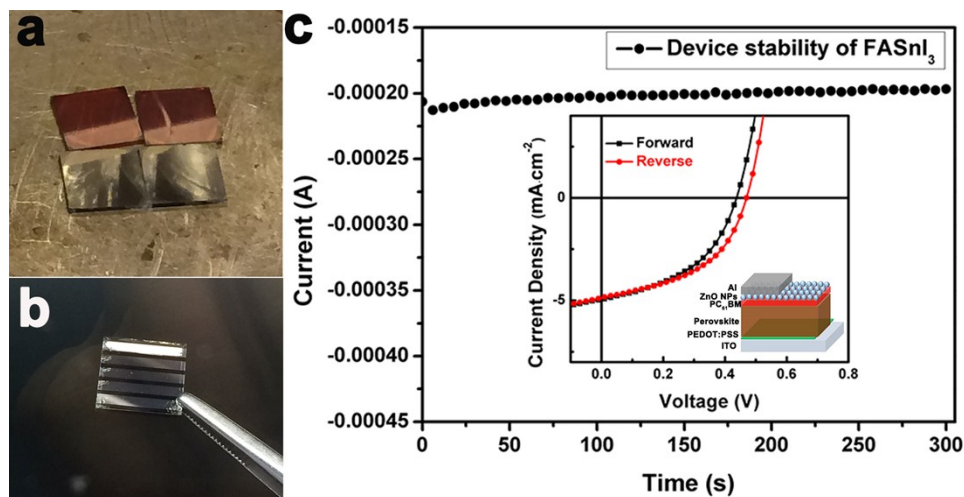


Figure S10. The pictures and PCE of FASnI_3 thin film devices based on the single-crystalline precursor solutions. (a) Brown FASnI_3 thin film based on the formation of SnI_2 combined with FAI in DMSO solvent; Black FASnI_3 thin film based on the single-crystalline precursors in DMSO solvent. (b) Fabrication of black FASnI_3 thin film solar cell device based on the single-crystalline precursors. (c) PCE and stability of black FASnI_3 planar solar cell based on the single-crystalline precursor; Insert: The device structure of FASnI_3 planar solar cell.

Table S1. Crystal structure parameters data of BA₂PbI₄.

Empirical formula	(n-C ₄ H ₉ NH ₃) ₂ PbI ₄
Formula weight/gmol ⁻¹	863.08
Temperature/K	293(2)
Crystal color	reddish
Wavelength/Å	0.71073
Crystal system	Orthorhombic
Space group	<i>Pbca</i>
<i>a</i> /Å	8.892
<i>b</i> /Å	8.713
<i>c</i> /Å	27.650
α /°	90
β /°	90
γ /°	90
Volume/Å ³	2142.3
<i>Z</i>	4
Density/g·cm ⁻³	2.676
μ (mm ⁻¹)	13.624
F (000)	1520
Crystal size (mm ³)	0.25 × 0.16 × 0.15
Reflection collected	1888
Independent reflection	1511
GOF on F ²	1.285
R ₁ , wR ₁ [<i>I</i> > 2σ (<i>I</i>)]	0.0571/0.1473
R ₂ , wR ₂ (all data)	0.0711 /0.1526
Min/Max Δρ /eÅ ⁻³	-1.374 /1.710
$w=1/[s^2(FO^2)+(0.0441P)^2+32.2000P]$ where $P=(FO^2+2Fc^2)/3$	

Table S2. The device parameters of black FASnI₃ planer solar cells based on the single-crytalline precursors.

Numbers		<i>V</i> _{OC} [V]	<i>J</i> _{SC} [mA·cm ⁻²]	<i>FF</i>	<i>PCE</i> [%]
1	Forward	0.44	4.95	0.46	0.98
	Reverse	0.47	4.87	0.47	1.08
2	Forward	0.39	4.25	0.39	0.66
	Reverse	0.40	3.89	0.44	0.70
3	Forward	0.39	3.83	0.46	0.71
	Reverse	0.40	4.48	0.41	0.75
4	Forward	0.30	2.62	0.35	0.28
	Reverse	0.33	2.66	0.39	0.35

References

- [1] Y. Dang, Y. Liu, Y. Sun, D. Yuan, X. Liu, W. Lu, G. Liu, H. Xia and X. Tao, *CrystEngComm*, **2015**, 17,665-670.